



# Monitoring the dressing operation of conventional aluminum oxide grinding wheels through damage index, power spectral density, and piezoelectric sensors

Erick Luiz Vieira Ruas<sup>1</sup> · Wenderson Nascimento Lopes<sup>2</sup> · Paulo Roberto de Aguiar<sup>1</sup> · Thiago Glissoi Lopes<sup>1</sup> · Pedro Oliveira Conceição Junior<sup>3</sup>

Received: 23 February 2023 / Accepted: 26 May 2023 / Published online: 7 June 2023  
© The Author(s), under exclusive licence to Springer-Verlag London Ltd., part of Springer Nature 2023

## Abstract

Monitoring the dressing operation of grinding wheels is crucial for optimizing the grinding process and ensuring quality outcomes. This study presents a novel data-driven method utilizing piezoelectric diaphragm signals, combined with the root mean square deviation index (RMSD) and power spectral density (PSD), to determine the optimal moment for interrupting the dressing operation of conventional aluminum oxide grinding wheels. By addressing the existing gaps in transition methods between dressed and undressed grinding wheels, as well as exploring untested metrics in digital signal processing, this research expands the use of alternative piezoelectric transducers for monitoring dressing. The proposed methodology utilizes a commercial acoustic emission (AE) sensor as a reference and employs experimental dressing tests to validate its effectiveness. The signals from both the AE sensor and the piezoelectric diaphragm are collected and subjected to digital processing to extract relevant features based on the proposed approach. Results demonstrate that the RMSD index successfully extracts information about the cutting surface conditions of the grinding wheel from signals obtained by both AE sensors and piezoelectric diaphragms. Furthermore, by selecting frequency bands that exhibit strong correlations with the grinding wheel's cutting surface conditions, a threshold is defined, enabling timely interruption of the dressing operation, thereby ensuring the restoration of the grinding wheel for continued use in grinding applications. Ultimately, this study showcases the feasibility of a non-invasive method for monitoring the dressing operation of conventional grinding wheels, contributing significantly to the optimization of the grinding process.

**Keywords** Dressing operation · Piezoelectric sensors · Damage index · Indirect monitoring

## 1 Introduction

Linked to the needs generated by increased competitiveness and an increasingly globalized market, manufacturing industries have been under pressure to increase levels

of productivity and quality. In the current scenario, manufacturing industries seek to replace processes that are very dependent on the skill of an operator, with alternatives that present greater predictability concerning the results of their activities. In this context, the grinding process and the dressing operation have received special attention from researchers in the manufacturing area.

In the manufacturing industry, grinding is one of the most common machining processes that is characterized by the removal of material by abrasion [1], where a tool called a grinding wheel is used, which is composed of abrasive grains linked by a binding material that is attached to a disc. The grinding wheel is coupled to a machine that passes it through the workpiece to be machined. The grinding wheel grains with different sizes and complex geometry are responsible for removing material from the surface of the workpiece during the grinding process.

✉ Pedro Oliveira Conceição Junior  
pedro.oliveiracjr@usp.br

<sup>1</sup> Department of Electrical Engineering, São Paulo State University (UNESP), Av. Eng. Luiz E. C. Coube, 14-01, Bauru, SP CEP: 17033-360, Brazil

<sup>2</sup> Paraná Federal Institute of Education, Science and Technology, Avenida Dr. Tito, 801, Jardim Panorama, Jacarezinho, PR CEP: 86400-000, Brazil

<sup>3</sup> Department of Electrical and Computer Engineering, São Carlos School of Engineering, University of São Paulo USP. Av. Trab. São Carlsruhe, 400 - Pq. Arnold Schimidt, São Carlos, SP CEP: 13566-590, Brazil

Grinding is often found in the last stages of mechanical manufacturing processes, increasing the need for error-free action. This occurs because the workpiece, in its final stage of manufacture, accumulates the added value of the previous stages of production [2, 3]. For the grinding process to meet technical requirements, such as the surface texture of the workpiece, roughness, and dimensional tolerances, the grinding wheel must present satisfactory cutting conditions. The proper condition of the grinding wheel is evaluated through its properties, such as a uniform cutting surface, without impurities and grains with cutting properties, among others.

The cutting properties of the grinding wheel decrease as a result of its use in the grinding process. This means that, after a specific moment, the grinding wheel does not meet the desired requirements to perform the proper finishing on the workpiece. Therefore, the dressing operation is used to restore the cutting properties and shape of the grinding wheel. The dressing operation consists of passing the wheel through a dresser (dressing tool), whose impurities, chips, and unclogging pores are removed, correcting possible flaws such as eccentricity and wear of the abrasive layer. Thus, the dressing operation is closely linked to the surface finish result of the machined workpiece, sustaining the slogan “grinding is dressing” [4, 5].

In the metalworking industry, monitoring the grinding process and the dressing operation largely depends on a qualified human operator [3]. Therefore, monitoring the grinding wheel cutting condition that can help the operator in decision-making is of great value for process optimization, as well as for the reduction of costs of production [6]. However, in the dressing operation, there is a great complexity for the monitoring and follow-up of events inherent to this action. This is due to the nature of the grinding wheel’s abrasive material. This tool is composed of grains with random shapes and sizes that are grouped by means of bonding material, making the cutting surface of the grinding wheel irregular and challenging to parameterize [7]. Therefore, researchers in the area face difficulties in proposing methods for monitoring the grinding wheel that can be generalized. In 1984, the subject was approached by Dornfeld and Cai [8], who, for the first time, used acoustic emission (AE) signals generated in the grinding processes to monitor and automate these actions with non-destructive and non-invasive tests, allowing data-driven monitoring in real-time assertively and systematically. Consequently, several studies have already addressed the use of AE to monitor the dressing operation, using the most varied mathematical tools for signal processing [7, 9–15]. In addition to the AE sensor, other sensors were used to collect the signals from the grinding process, as in [10], which used a low-cost piezoelectric transducer, also known as a piezoelectric diaphragm, for the same monitoring scope.

Although both sensors (AE and piezoelectric diaphragm) can evaluate the same event, it cannot be predicted that they will present the same response in detecting event signals, as each one has a particular physical structure and frequency response. However, despite different structures and compositions, the responses of the signals can be treated similarly, applying mathematical and statistical tools to them to extract the most sensitive features related to the grinding process [7]. Signal processing techniques, such as event counts, root mean square (RMS), short-time Fourier transform (STFT), signal energy, fast Fourier transform (FFT), and power ratio (ROP), have been used in the development of data-driven methods for monitoring the dressing operation [9, 12]. Thus, the present research work aims to present a new approach based on the AE sensor and piezoelectric diaphragm, as well as on power spectral density (PSD) and RMSD index to determine the appropriate moment to interrupt the dressing operation of conventional grinding wheels.

It is noteworthy that the present research differs from other literature studies in the following key aspects and contributions: (i) the RMSD index has not yet been investigated as an alternative for the composition of non-invasive methods for monitoring the dressing operation of conventional grinding wheels; (ii) the RMSD index has not yet been used to extract the characteristic of signals generated by piezoelectric sensors during the dressing operation, such as AE sensors and piezoelectric diaphragms. In this context, the present study aims to fill the existing gap in approaches that determine the appropriate time of transition between the conditions of the dressed and undressed grinding wheel, seeking to advance the knowledge about the conditions of the grinding wheel in the dressing process from AE signals generated with the piezoelectric diaphragm, which presents itself as an alternative transducer and has been increasingly used in the composition of methods for monitoring the grinding process [16–18]. This work also aims to contribute to selecting the appropriate frequency bands related to the grinding wheel condition, establishing an optimal threshold that can be used to interrupt the dressing operation at the proper time.

## 2 State of the art

This section will be divided into three sub-items: (i) a brief review of the literature that addresses the dressing operation, covering the main variables of the process, (ii) dressing monitoring using AE sensors and the piezoelectric diaphragm, and (iii) overview on the PSD and RMSD representative metrics used in the proposed approach.

### 2.1 Dressing operation

The dressing operation aims to restore the grinding wheel cutting condition after the wear resulting from its use in the grinding process [19]. Among the dressing techniques, the one that uses the single-point dresser is the simplest and is used on a large scale in manufacturing environments for dressing conventional grinding wheels [6, 20]. However, using a single-tip dresser requires some dressing parameters to be defined to guarantee satisfactory performance of the dressing action. These parameters are the width of the dresser tip represented by  $b_d$ , the dressing step  $S_d$ , the dressing time  $t_d$ , and the dressing overlap ratio  $U_d$ , as shown in Fig. 1.

Dressing conventional grinding wheels using single-point dressers produces two effects on the grinding wheel surface: (i) macro effect and (ii) micro dressing effect. The macro dressing effect is due to the shape of the thread printed on the grinding wheel when going through the dressing operation using the single-point dresser. The micro effect, however, is generated on the grinding wheel’s cutting surface due to the fractures caused by the dresser in the abrasive grains and the bounding material. These two types of effects are directly related to the dressing overlap ratio parameter ( $U_d$ ). The overlap ratio describes the effective dressing width ( $b_d$ ) with the displacement of the tool along the cutting surface of the grinding wheel, which is called dressing pass ( $S_d$ ). The parameter  $U_d$  significantly influences the sharpness of the grinding wheel and must be determined according to the intensity of material removal desired during the grinding of the workpiece [21, 22].

The primary method to quantify the sharpness of the grinding wheel is called the “ground disc method” presented by Moia [23], which consists of a fixed disc connected to a balance system and, without rotation, pressed with a constant normal force against the surface of a grinding wheel. As the wheel performs an angular displacement, the disc travels along the cutting surface of the wheel, which removes material from the wheel. In contrast, the other end of the balance performs a vertical movement measured using an electronic probe, which converts the displacement into an electrical signal. Subsequently, using Eq. (1), the sharpness of the grinding wheel can be determined.

$$K = \frac{2b\sqrt{8r}}{3F_n} \times (a)^{2/3} \tag{1}$$

where  $b$  is the width of the grinding wheel,  $r$  represents the radius,  $F_n$  is the applied normal force, and  $a$  is the gradient of the regression line obtained from the experimental displacement characteristic.

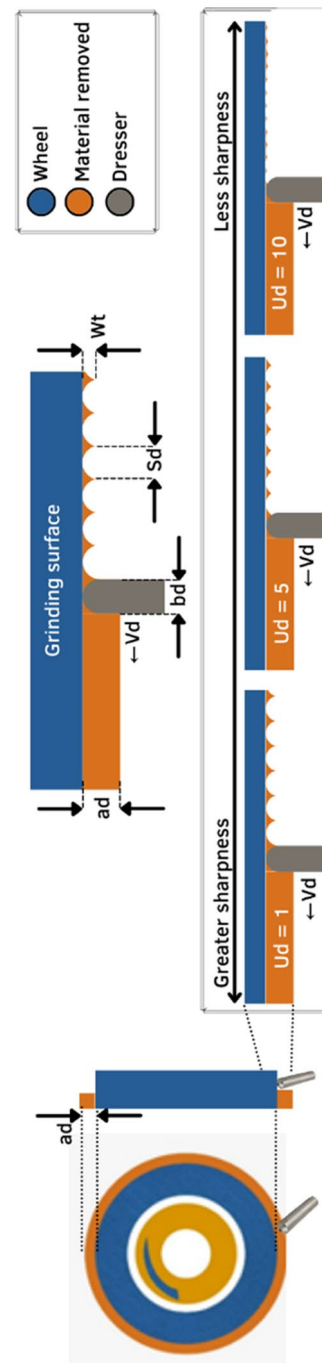


Fig. 1 Dressing process with a single-point dresser

## 2.2 Dressing monitoring

Sensor monitoring of the grinding wheel condition through acoustic emission has been the subject of study since 1984 [8]. Furthermore, because of reducing manufacturing costs and optimizing both the grinding process and the dressing operation, monitoring the grinding wheel's cutting surface is a scientific topic that still needs investigation. The development of studies to analyze the conditions of the grinding wheel during the dressing operation allows for an evaluation in real time of the quality of the condition of the cutting surface of the tool. In this way, it is possible to infer an optimal point to stop the operation, which increases tool life as well as savings in production costs.

AE signals have been widely used for several monitoring scopes in the grinding process, as in [8], which used the root mean squared value (RMS) for feature extraction in the dressing process, and in [19], which used AE in the monitoring of both dressing and grinding operations. The authors of [20] present a broad study focusing on the data-driven classification of wear levels of single-point dressers through AE signals. The ratio of power (ROP) and root-mean-square (RMS) statistics were applied, and the results were used as inputs into two distinct neural models based on the multilayer perceptron (MLP) and Kohonen self-organizing neural networks. The results obtained by the authors showed satisfactory performance in classifying the wear level of single-point dressers. Furthermore, the study developed in [24] shows a satisfactory result for the use of AE to identify changes in the grinding wheel during its use in the grinding process, as well as to detect grinding burn through the decomposition of AE signals, establishing an automated classification system.

In [25], the authors present a study focused on dressing operation in cylindrical grinding (centerless) using the Tamaguchi method and load cells. It demonstrated a cycle time reduction of the dressing operation, causing, consequently, an increase in the productivity of the process under study. Furthermore, using the Tamaguchi method and load cells allowed a better understanding of the dynamics of the dressing operation, resulting in an effective diagnosis of the operation and helping to identify problems in the grinding devices. In this study, the authors used the cutting speed, dressing depth, feed rate of the dresser, and diameter of the grinding wheel as grinding parameters. In the work of [13], the authors present the prediction of the wear level of the single-point dresser from AE and vibration signals, using them as input variables for a *Fuzzy* model. For this, AE and vibration sensors were attached to the tool holder, and the signals were recorded at a sampling frequency of 2 MHz. Subsequently, digital filters were applied to the raw signals, and two statistics were calculated to serve as inputs for the *Fuzzy* models. The results indicate that the *Fuzzy* models

effectively predict the wear level of the dresser. AE to monitor the dressing process is also found in the work of [23], in which these signals were used to classify the condition of the tool through artificial neural networks (ANN). Several statistical methods, such as the RMS, were applied to the raw signal, and the result was used as input to a multilayer perceptron neural network. The results presented were satisfactory in identifying the tool's cutting capacity.

The work developed by [11] studies the feasibility of using a low-cost piezoelectric diaphragm as an alternative to traditional AE sensors in monitoring the dressing process of aluminum oxide grinding wheels. The feasibility study employed both time and frequency domain analyses. Through analysis in the frequency domain, the authors found a correlation above 90% between the piezoelectric diaphragm and AE sensor signals when analyzed in a specific frequency range. Furthermore, the work developed by [12] proposed a method for fault diagnosis on the cutting surface of aluminum oxide grinding wheels in the grinding process. The proposed method employs the short-time Fourier transform (STFT) analysis in the time–frequency domain and the ROP metric. As a result, the authors proposed the wheel shape factor (WSF) parameter, which proved to be effective in quantifying the topographic uniformity of the cutting surface of conventional aluminum oxide grinding wheels. Time–frequency domain analysis was also used in the article developed by [9], who proposed an algorithm cooperating with STFT for grinding wheel condition monitoring through AE signals. The algorithm proposed by the authors employs analyses that include using the correlation coefficient deviation metric (CCDM) damage index to find the best parameters to calculate the STFT. Other authors, such as [2, 20, 23, 26], and [27], also used the AE to monitor the grinding process or the dressing operation.

## 2.3 Digital signal processing tools

When the data contains no random effects or noise, it is called deterministic. In this case, one computes a Fourier transform. One computes a power spectrum when random effects obscure the desired underlying phenomenon. According to [28], the power spectrum or power spectral density (PSD) reveals the existence, or the absence, of repetitive patterns, vibrations, and correlation structures in a signal process. These structural patterns are essential in a wide range of applications, such as data forecasting, signal coding, signal detection, radar, pattern recognition, and decision-making systems. The most common method of spectral estimation is based on the fast Fourier transform (FFT). For many applications, FFT-based methods produce sufficiently good results. However, more advanced methods of model-based spectral estimation can offer better frequency resolution and less variance.

One of the most used methods for estimating PSD is the Welch method, based on the periodogram estimation method developed by Bartlett. Welch altered Bartlett’s periodogram by introducing the overlap of segments and windowing each segment of the original sequence [29]. He also raised the possibility of using a window other than the rectangular one to analyze the periodogram, which resulted in a modified periodogram. Several works in manufacturing process monitoring that used the Welch method can be found, such as in [15, 30]; the PSD combined with the deviation of the mean squared value (RMSD—referred to as damage index) gave rise to a new methodology proposed by [7] to monitor the burning phenomenon in the grinding process.

The RMSD index is a metric used to compare signals, verifying the existing variations between the signal that represents the baseline and the other collected signals. In [27], the RMSD is calculated based on the Euclidean norm, which can be found in several forms in the literature. The RMSD result is greater than or equal to zero, with zero representing the exact equality of the signals compared to the baseline. The RMSD is calculated by Eq. (2):

$$RMSD = \sum_{k=\omega_l}^{\omega_f} \sqrt{\frac{[X_D(k) - X_H(k)]^2}{X_H^2(k)}} \tag{2}$$

where  $X_H$  is the signal in initial conditions,  $X_D$  is the signal of the damaged condition, and  $k$  is a frequency band that varies from  $\omega_l$  (initial frequency) to  $\omega_f$  (final frequency).

### 3 Material and methods

To achieve the objectives proposed in this study, dressing tests were performed in a surface tangential grinding machine, model RAPH 1055 from Sulmecânica, which was equipped with an aluminum oxide grinding wheel, from NORTON, model 38A.100.LVH, with an initial dimension of 352.8 × 25.4 × 127 mm. Figure 2 shows the distribution scheme of the components used in the dressing tests. In the tests, a single-point diamond dresser was

used, obtained by the chemical vapor deposition (CVD) technique. Coupled to the dresser support, an AE sensor is manufactured by the company Sensis and a low-cost piezoelectric diaphragm, model 7BB-35-3, from the company Murata Electronics, which were used to capture the acoustic waves generated by the contact between the surface of grinding wheel and the dresser tip. For conditioning, the signals were generated by the AE sensor, and a module from the manufacturer Sensis, model DM-42, was used. It should be noted that the signals acquired by the piezoelectric diaphragm were not conditioned, connecting it directly to the oscilloscope. The signals generated in the tests were collected simultaneously at a sampling frequency of 2 MHz using a Yokogawa model DL850 oscilloscope.

#### 3.1 Setting the dressing parameters

The dressing parameters were configured to perform two sets of tests: (i) one to demonstrate the method and (ii) another to verify the method. For comparative purposes, the tests were defined with controlled dressing parameters. The parameters involved in the dressing tests are the wheel rotation speed  $N_s$ , the wheel diameter  $D_s$ , the wheel peripheral speed or cutting speed  $V_s$ , the dressing depth  $a_d$ , effective dressing width  $b_d$ , the dressing time  $t_d$ , the dressing overlap ratio  $U_d$ , and, finally,  $S_d$  which is called the dressing step. The parameters adopted in the method demonstration test are shown in Table 1, while Table 2 shows the parameters adopted in the method verification test. Notably, the acronym  $P_d$  represents the number of dressing passes performed in each dressing test.

To measure the effective dressing width ( $b_d$ ), a digital microscope of the brand DTN, USB model DNT DigiMicro 2.0 Scale, with a camera of two megapixels of resolution, was used. The microscope software made it possible to measure the diamond tip of the dresser from the captured images. To maintain the proportions, the photos were always captured from the same position, at 8 mm from the tip of the dresser, using the body of the dresser, which corresponds to 10 mm in diameter, as a reference.

Fig. 2 Distribution diagram of the components used in the tests

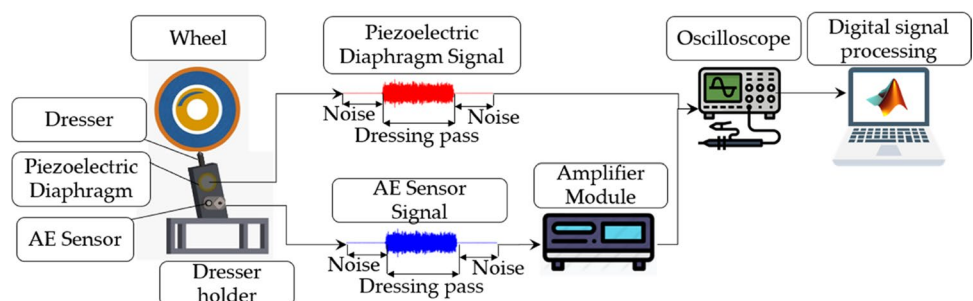


**Table 1** Dressing test parameters for method demonstration

Parameters involved in dressing tests							
$N_s$ [RPM]	$D_s$ [mm]	$V_s$ [m/s]	$b_d$ [ $\mu$ m]	$t_d$ [s]	$S_d$ [mm]	$U_d$	$P_d$
1800	351.6	33.14	522	5675	0.1491	3.5	25

### 3.2 Execution of dressage tests

The tests consisted of 25 passes of the diamond tip of the dresser across the cutting surface of the wheel, thus removing 25 layers of abrasive material from the cutting surface of the wheel in each test performed. The sequence of execution of the tests was arranged in the following steps:

- (i) In order to degrade the cutting surface of the grinding wheel, before the dressing test, the grinding wheel was used in the process of severe grinding of ABNT 1020 steel workpiece, with dimensions  $150 \times 48 \times 12$  mm. In this process, 20 passes of the grinding wheel were performed on the surface of the workpiece, at a cutting depth of  $20 \mu\text{m}$  and table speed of approximately  $44 \text{ mm/s}$ , without the use of cutting fluid.
- (ii) Then, images of the cutting surface of the grinding wheel were collected with a digital microscope and a smartphone from Samsung, model Galaxy J2, equipped with a five-megapixel camera and a resolution of  $2592 \times 1944$  pixels.
- (iii) Next, before starting the dressing operation, the ground disc method was used to measure the sharpness of the grinding wheel in 03 (three) positions along its cutting surface, thus obtaining the average sharpness of the tool.
- (iv) Soon after, with the grinding wheel's cutting surface degraded, the dressing test was started using cutting fluid and  $a_d$  equal to  $10 \mu\text{m}$ . After 5, 10, and 25 dressing passes, the test was interrupted, and then measurements of the sharpness of the grinding wheel were carried out in 3 positions along its cutting surface, and subsequently, an average sharpness was obtained. Finally, at the end of the test (after 25 passes), images of its cut surface were captured using the digital microscope and smartphone.

It is noteworthy that following these steps, two sets of dressing tests were performed, keeping the  $a_d$  constant and equal to  $10 \mu\text{m}$ . However, with different values for the

parameter  $U_d$  being (i) the first test performed with  $U_d$  equal to 3.5 in order to demonstrate the method and (ii) the second test performed with  $U_d$  equal to 5.5 to verify the proposed method.

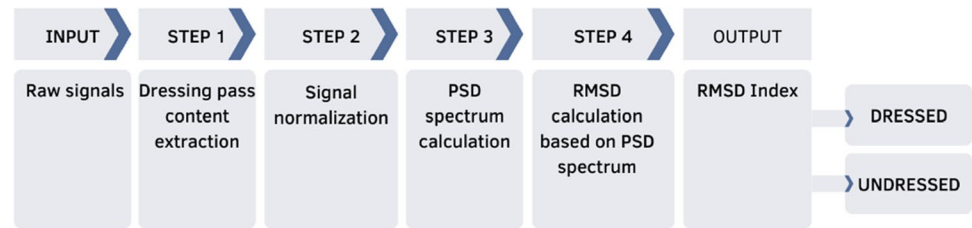
### 3.3 Proposed method for monitoring the dressing operation through the damage index

After performing the dressing tests, the collected signals referring to the AE sensor and the piezoelectric diaphragm were processed in the MATLAB® software. These signals, which have not yet undergone any type of treatment, are defined as original or raw signals composed of a noise signal (before wheel-dresser engagement), a signal referring to the dressing pass, and a noise signal (after the dresser leaves the wheel), with the noise signal being an acoustic characteristic of the industrial environment that involves machine vibrations, wheel rotation, and machine tool feeding, among others. From these original signals, as shown in Fig. 3, four digital processing steps were performed: (i) only the signals corresponding to the dressing pass were selected, eliminating noise before the rising edge and after the falling edge [30]; (ii) later, the signals were normalized by dividing them by their respective maximum values; (iii) then, applying the Welch method with an overlap of 50%, the PSD of all normalized signals were computed; (iv) finally, using as a baseline the frequency spectrum obtained for the twenty-fifth dressing pass, which represents the grinding wheel in the dressed condition, the RMSD indices were computed using a sliding window of length equal to 10 kHz, starting at 2 kHz and ending at 200 kHz, that is, for each frequency band, 25 values are obtained for the RMSD index. These steps are exemplified in Fig. 3, with the final output being the classification of the grinding wheel as dressed or undressed, depending on the values observed for the RMSD index. It should be noted that both the signals referring to the method demonstration test and the signals referring to the method verification test were processed according to the steps shown in Fig. 3 and described in topic 3.3.

**Table 2** Dressing test parameters for method verification

Parameters involved in dressing tests							
$N_s$ [RPM]	$D_s$ [mm]	$V_s$ [m/s]	$b_d$ [ $\mu$ m]	$t_d$ [s]	$S_d$ [mm]	$U_d$	$P_d$
1800	351.2	33.1	684	6.81	0.1244	5.5	25

**Fig. 3** Sequence applied to the treatment of data obtained both in the demonstration test and in the method verification test



This process was carried out to identify the best frequency range that should be used to characterize the conditions of the grinding wheel through the RMSD index and, thus, define the appropriate moment to interrupt the dressing operation, ensuring that the grinding wheel is suitable for use in the grinding process. It is worth emphasizing that the study also seeks to determine a threshold that makes it possible to classify the grinding wheel as dressed or undressed. The definition of this threshold allows the implementation of a robust and reliable control system to assist the operator in decision-making.

## 4 Results and discussion

This section is divided into three main topics: 4.1, where the results obtained for the method demonstration are presented and discussed; 4.2, where the results obtained for the method verification are presented and discussed; and finally, 4.3 where the results obtained for both dressing tests are compiled and discussed.

### 4.1 Results obtained from the dressing test for the demonstration of the method

To demonstrate the conditions of the grinding wheel, Fig. 4a exposes the grinding wheel's cutting surface in its undressed condition, that is, before starting the dressing process. Figure 4b shows the cutting surface of the grinding wheel after finishing the dressing operation.

The cutting surface of the grinding wheel shown in Fig. 4a contains residues that promote clogging, mainly covering the abrasive grains of the grinding wheel, which significantly interferes with its sharpness, contrary to what is shown in Fig. 4b, where it is possible to verify a uniform distribution of abrasive grains, pores, and binders, making the cutting surface of the grinding wheel more homogeneous and aggressive. In Fig. 5, when measuring the sharpness ratio of the grinding wheel's cutting surface, with the amount of material removed from the grinding wheel during the dressing passes, it is possible to notice that there is a tendency towards normalization in sharpness.

This normalization, which can be observed from 1400 mm<sup>3</sup> of material removed from the grinding wheel's cutting surface, means that even removing more abrasive layers from the grinding wheel, the sharpness of its cutting surface does not change significantly. This characterizes that after 1400 mm<sup>3</sup>, the dressing operation has already reached its purpose, producing a regular and sharp cutting surface, thus being able to infer that the grinding wheel is dressed. These results were similar to the results obtained by Lopes et al. [22].

During the dressing test, the acoustic activity was captured by piezoelectric sensors, and a significant difference can be observed between the signals generated for the conditions of dressed and undressed grinding wheel. Figure 6 shows the original signals captured in the method demonstration. These signals were amplitude normalized and are related to the condition of the dressed and undressed grinding wheel. Figure 6a refers to the signals collected with the AE sensor, and Fig. 6b refers to the signals collected with the piezoelectric diaphragm. The signals presented in Figs. 6a and b, respectively, in blue and black, refer to the

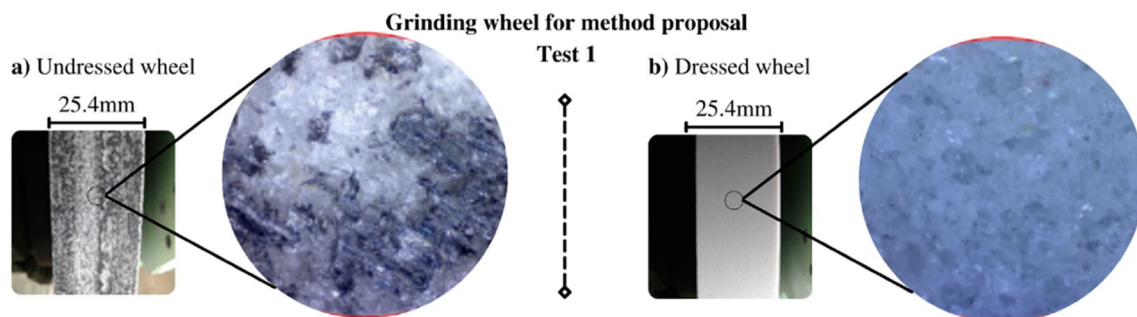
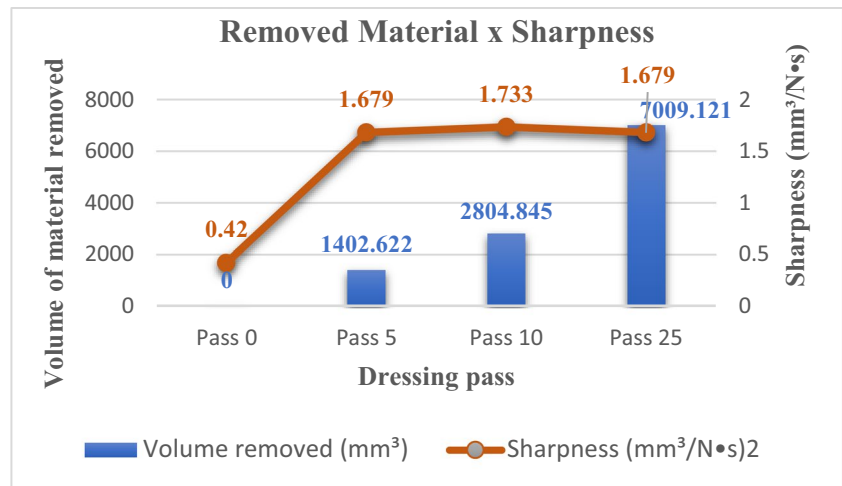


**Fig. 4** The cutting surface of the grinding wheel

**Fig. 5** Sharpness versus volume of material removed from the method demonstration



condition of the undressed grinding wheel, that is, to the first dressing pass. On the other hand, the signals shown in red and yellow, respectively, in Fig. 6a and b, are related to the condition of the dressed grinding wheel. In the signals representing the condition of the undressed grinding wheel, it is possible to identify that the amplitudes behave in an oscillatory way along the dressing pass. This characterizes that the grinding wheel's cutting surface is degraded and not uniform.

On the other hand, in relation to the signals presented in red and yellow, respectively, in Fig. 6a and b, along the dressing pass, it is noticeable that there is uniformity in the amplitude of the signals, configuring that at that moment, the surface grinding wheel is more even and provides a more uniform contact between the grinding wheel and the dresser. However, this transition is not easily noticed by the operator since, at present, this monitoring is done visually and audibly and requires specific experience and human skills. And in many cases, the ideal frequencies for monitoring the dressing operation are above the range of frequencies humans can hear. As is the case of this study, when obtaining the frequency curves via PSD, it

is observed in Fig. 7 that for both the AE sensor and the piezoelectric diaphragm, the frequency range that presented the best result is significantly above 20 kHz. Furthermore, it is observed in Fig. 7a that the frequency range that extends from 182 to 192 kHz, selected for the AE sensor, has amplitudes different from the frequency range specified for the piezoelectric diaphragm, which extends from 168 to 178 kHz, which is presented in Fig. 7b. Still, in Fig. 7, when comparing the frequency curve obtained for the undressed grinding wheel with the frequency curve obtained for the dressed grinding wheel for both sensors, it is noted that there is a significant difference between the amplitudes of these frequency curves. Thus, for both sensors, when analyzing the frequency curves visually, it is possible to classify the wheel as dressed and undressed since the frequency curves obtained for the dressed wheel present amplitudes with a significant difference when compared to the amplitudes of the curves of frequencies obtained for the grinding wheel in the undressed condition.

This difference between the amplitudes of the frequency curves obtained for different conditions of the grinding wheel's cutting surface is even more visible when obtaining

**Fig. 6** Raw signals referring to the method demonstration test: **a** AE sensor and **b** piezoelectric diaphragm

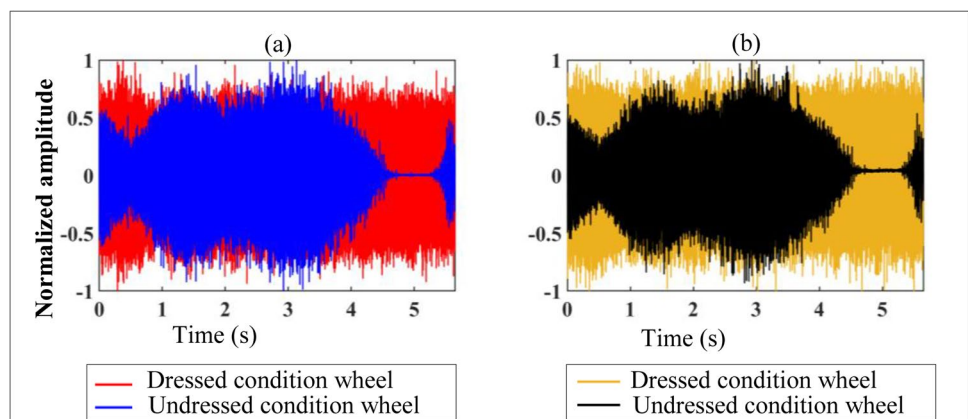
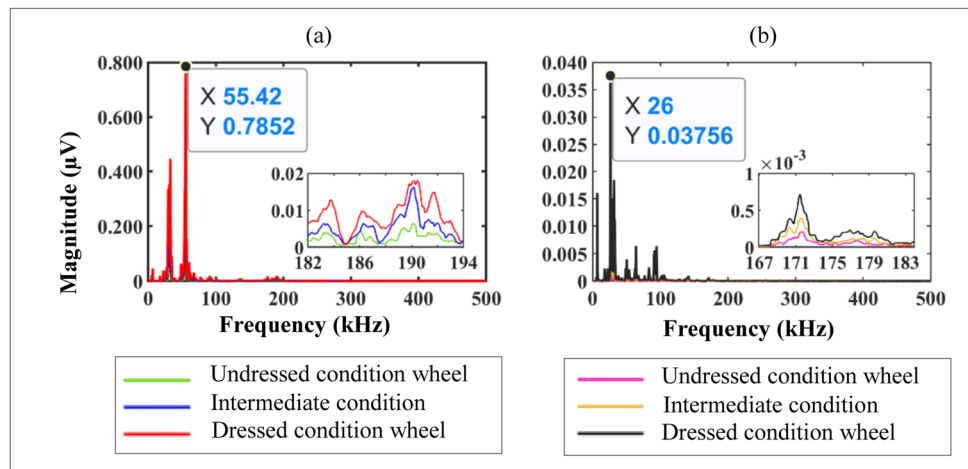




**Fig. 7** PSD spectra of the original signals referring to the method demonstration test: **a** AE sensor and **b** piezoelectric diaphragm



the damage index values through the RMSD metric. Note in Fig. 8 that, for both sensors, the RMSD index is sensitive to amplitude variations of the frequencies that best characterize the cutting conditions of the grinding wheel. It can also be seen in Fig. 8 that, for the AE sensor, the damage index obtained for the wheel in the dressed condition is 274% lower than the damage index obtained for the undressed wheel condition. As for the piezoelectric diaphragm, the damage index obtained for the grinding wheel in the dressed condition is 245% lower than that obtained for the undressed grinding wheel condition. It is also observed in Fig. 8 that for the undressed grinding wheel condition for both the AE sensor and the piezoelectric diaphragm, the damage indexes are far above zero.

On the other hand, for the dressed wheel condition, for both sensors, the damage index approaches zero. Suppose the value of the RMSD index is equal to zero when defining the frequency curve that represents the dressed grinding wheel as a baseline. In that case, it means that the frequency

curve obtained is exactly equal to the selected baseline for the dressed grinding wheel condition. However, for this methodology, the damage indices approach zero, but they will hardly be exactly zero since, during the dressing operation, it is impossible to collect two signals the same since the process is stochastic and has many variables that significantly influence the signals generated during dressing. Thus, by defining the frequency curve related to the condition of the dressed grinding wheel as a baseline, it is possible to obtain damage index values that make it possible to classify the grinding wheel as dressed and undressed.

#### 4.2 Results obtained from the dressing test for method verification

Regarding the method verification, in an identical way to the first set, the images of the grinding wheel were captured in both dressed and undressed conditions. The cutting surface of the grinding wheel shown in the image in Fig. 9a contains residues that promote clogging, mainly covering the abrasive grains of the grinding wheel, which interferes with the sharpness of the grinding wheel, contrary to what is shown in Fig. 9b, where it is possible to see a uniform distribution of abrasive grains, pores, and binders, making the cutting surface more homogeneous and aggressive.

Due to the degradation caused on the cutting surface of the grinding wheel, Fig. 9a, its sharpness was significantly reduced to an approximate value of  $0.20 \text{ mm}^3/\text{N}\cdot\text{s}$ , as shown in Fig. 10. Under these conditions, if the grinding wheel is used in the grinding process, it can cause irreparable damage to the surface of the workpiece. It can be seen in Fig. 10 that after removing  $1400 \text{ mm}^3$  of abrasive material from the grinding wheel's cutting surface, its sharpness increased by approximately 770%. This means that the cutting ability of the abrasive grains has been restored. This significant increase in the sharpness of the grinding wheel also attests to the removal of unwanted material from its surface,

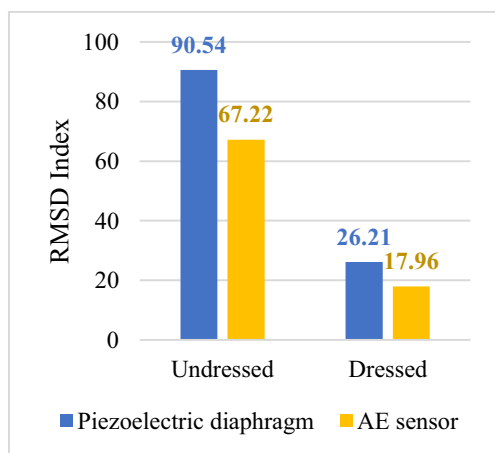


**Fig. 8** RMSD index refers to the method demonstration

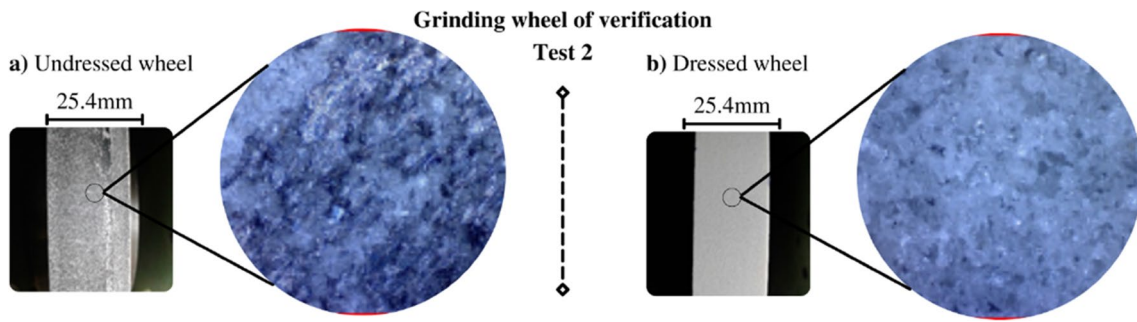


Fig. 9 The cutting surface of the grinding wheel used for method verification

besides the micro and macro effects produced by the dressing operation.

It is also observed in Fig. 10 that from 1400 mm<sup>3</sup> of material removed, there is not such a significant difference in the sharpness of the grinding wheel, which suffers slight variation. This means that if the grinding wheel has a smooth cutting surface after 1400 mm<sup>3</sup> of material is removed, the dressing operation has reached its intended purpose and can be stopped. Finally, concerning the condition of the dressed grinding wheel, it is noted that for U<sub>d</sub> equal to 5.5, the sharpness of the grinding wheel is lower when compared to the values obtained for U<sub>d</sub> equal to 3.5 used in the demonstration test of the method.

As occurred for the method demonstration, Fig. 11 shows the original signals, normalized in amplitude, related to the condition of the dressed and undressed grinding wheel. Figure 11a refers to the signals collected with the AE sensor and Fig. 11b to the signals collected with the piezoelectric diaphragm. The signals shown in Fig. 11a and b, respectively, in blue and yellow, refer to the undressed grinding wheel condition, that is, to the first dressing pass. On the other hand, the signals shown in red and black, respectively, in Fig. 11a and b, are related to the condition of the dressed grinding wheel.

It is observed in Fig. 11 that the same behavior was reported for the signals collected in the method demonstration. It is also noted that along the dressing pass that represents the condition of the undressed grinding wheel, for both sensors, the signal amplitudes behave irregularly over time. On the other hand, it is clearly perceived that there is greater uniformity in the amplitudes of the signals related to the conditions of the dressed grinding wheel, which are presented in red and black in Fig. 6a and b, respectively.

When analyzing these signals in the frequency domain, it is observed in Fig. 12 that for both the AE sensor and the piezoelectric diaphragm, the most significant harmonic content of the dressing operation is below 200 kHz. As observed in the frequency curves obtained for the method demonstration, it is noted in Fig. 12a that the frequency range that extends from 182 to 192 kHz selected for the AE sensor has amplitudes different from the frequency range specified for the piezoelectric diaphragm, which extends from 168 to 178 kHz and is shown in Fig. 12b. Still, in Fig. 12, when comparing the frequency curve obtained for the undressed grinding wheel with the frequency curve obtained for the dressed grinding wheel for both sensors, it is noted that there is a significant difference between the amplitudes of the frequency curves. This means that despite the variation in dressing parameters, the selected frequency bands

Fig. 10 Sharpness versus volume of material removed from the method verification

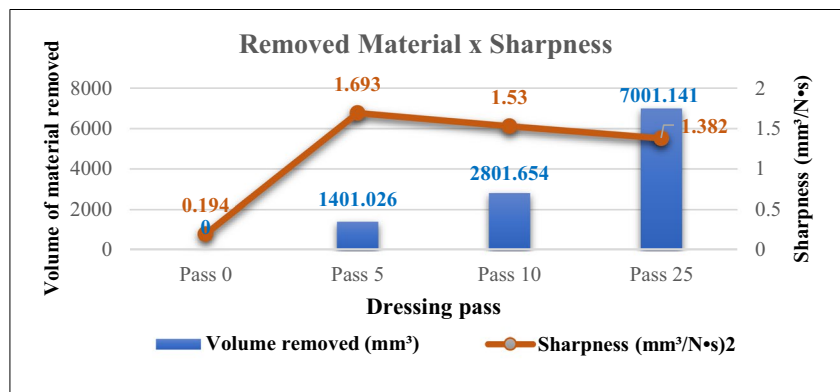
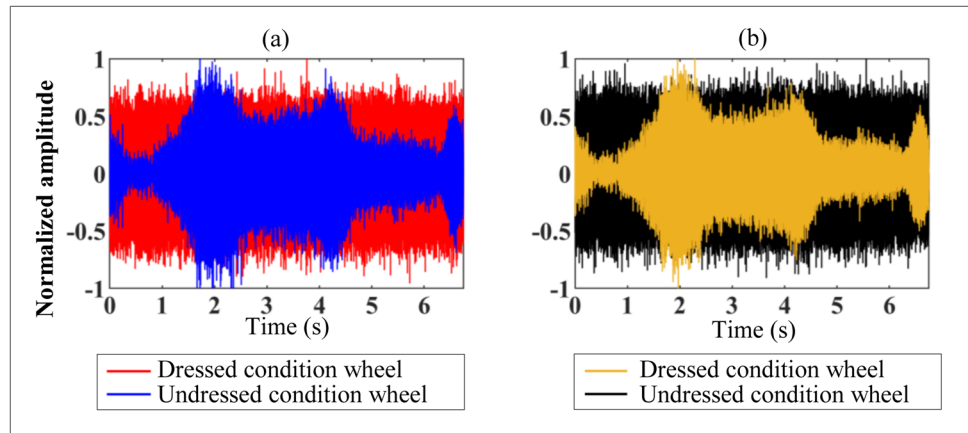


**Fig. 11** Raw signals referring to the method verification: **a** AE sensor and **b** piezoelectric diaphragm



are directly related to the cutting conditions of the grinding wheel. This relationship is highlighted by obtaining the damage indices computed via the RMSD metric.

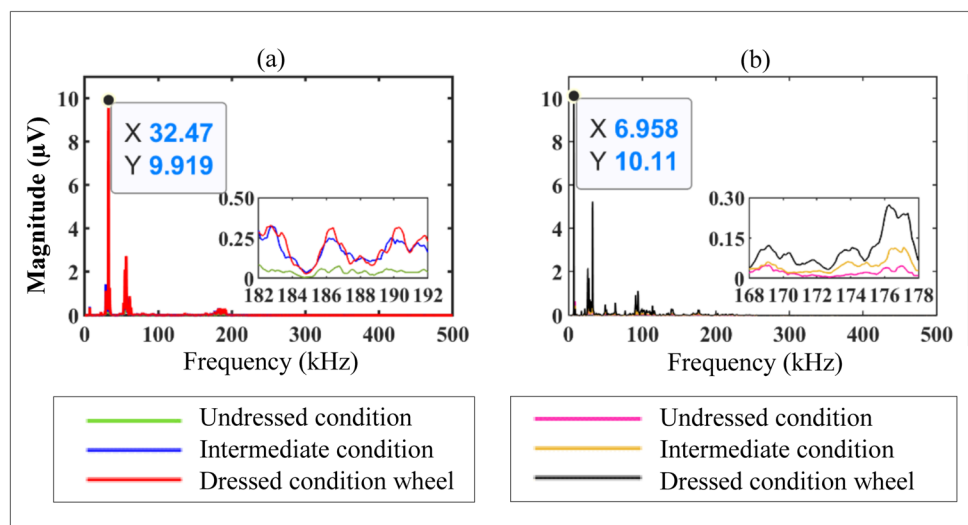
As was the case for the demonstration test of the method concerning the AE sensor, it can be seen in Fig. 13 that the damage index obtained for the grinding wheel in the dressed condition is 244% lower than the damage index obtained for the undressed grinding wheel condition. As for the piezoelectric diaphragm, the damage index obtained for the grinding wheel in the dressed condition is 366% lower than that obtained for the undressed grinding wheel condition.

Still, in Fig. 13, as was observed for the method demonstration, it appears that the damage indexes are far above zero for the undressed grinding wheel condition for both the AE sensor and piezoelectric diaphragm. It is observed that the frequency range that extends from 182 to 192 kHz selected for the AE sensor, for both methods of demonstration and verification, presented consistent

results in classifying the grinding wheel as dressed and not dressed. It is also noteworthy that the same analysis can be performed for the piezoelectric diaphragm when selecting the frequency range that extends from 168 to 178 kHz. Similar to the results obtained through the signals captured with the AE sensor, the results computed from the signals collected through the low-cost piezoelectric diaphragm were consistent in classifying the grinding wheel as dressed or undressed.

Finally, when comparing the damage index values obtained for the dressed grinding wheel condition with the damage indices obtained for the undressed grinding wheel condition, a difference greater than 200% is observed for both the AE sensor and piezoelectric diaphragm. This difference can be observed in the method demonstration as well as in the method verification. This attests that the results obtained for the low-cost piezoelectric diaphragm are as consistent and robust as the results obtained using the significantly more expensive AE sensor.

**Fig. 12** PSD spectra of the original signals referring to the method verification test: **a** AE sensor and **b** piezoelectric diaphragm



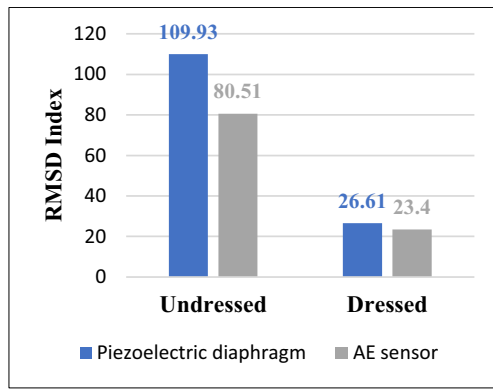


Fig. 13 RMSD index corresponding to the method of verification

### 4.3 Compilation of results

The method proposed in this research requires a frequency range that best characterizes the grinding wheel cutting conditions to be selected and a baseline to be used for comparison purposes. In this case, the most appropriate baseline must represent the grinding wheel in its full condition, ready to be used in the grinding process without causing damage to the workpiece. Throughout the research, it was observed that many frequency bands do not have a direct relationship with the cutting conditions of the grinding wheel. Figures 14 and 15 show the damage rates obtained through the RMSD metric, both for the data obtained in the method demonstration and for the data collected in the method verification. In Fig. 14, the damage indices obtained for the AE sensor are presented, and Fig. 15 shows the damage indices computed from the signals generated by the piezoelectric diaphragm.

In Fig. 14a and 15a, the damage indices obtained for frequency bands that are not directly related to the grinding wheel cutting conditions are presented. For the AE sensor, the frequency range that extends from 80 to 90 kHz was selected, and the frequency range that extends from 40 to

50 kHz was selected for the piezoelectric diaphragm. It is observed that the RMSD indices presented in Figs. 14a and 15a behave randomly. This result does not make it possible to classify the grinding wheel as dressed or undressed. Using these frequency ranges, it is not possible to define at what point the grinding wheel has its cutting condition reestablished, nor does it allow to determine a threshold that can be used to determine the appropriate moment to interrupt the dressing operation.

On the other hand, in Figs. 14b and 15b, the damage indices obtained for frequency bands that are directly related to the grinding wheel cutting conditions are presented. For the AE sensor, the frequency range that extends from 182 to 192 kHz was selected, and for the piezoelectric diaphragm, the frequency range that extends from 168 to 178 kHz was selected. It is observed that for both sensors, the damage rates shown in Figs. 14b and 15b have a well-defined trend and make it possible to clearly identify the values that are related both to the condition of dressed grinding wheel and to the condition of the undressed grinding wheel. For the first dressing pass, it is also noted in Figs. 14b and 15b that the computed damage indices are significantly far from zero, and throughout the dressing operation, these damage indices approach zero and tend to be stable. It is also noted that after the tenth dressing pass, approximately 2800 mm<sup>3</sup> of material was removed from the grinding wheel's cutting surface. The damage rates do not suffer significant variations. This stability means that the dressing has achieved its purpose, that is, the grinding wheel has a uniform cutting surface, and its sharpness is restored.

It is crucial to emphasize that before the dressing operation, the grinding wheel exhibited a damaged, irregular, and non-aggressive cutting surface. To assess the extent of damage, a reference signal representing the condition of a dressed grinding wheel was employed. This implies that both the AE sensor and the piezoelectric diaphragm exhibit similar frequency behavior in the collected signals

Fig. 14 RMSD index for the signals collected through the AE sensor: (a) 80–90 kHz; (b) 182–192 kHz

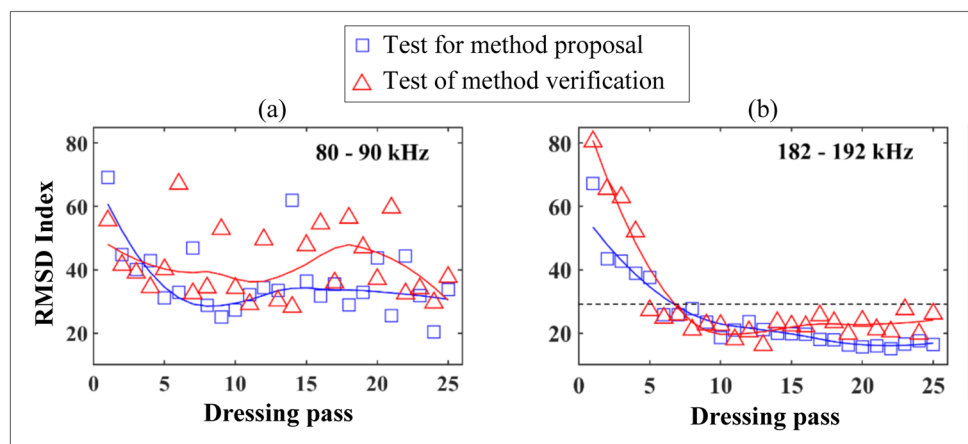
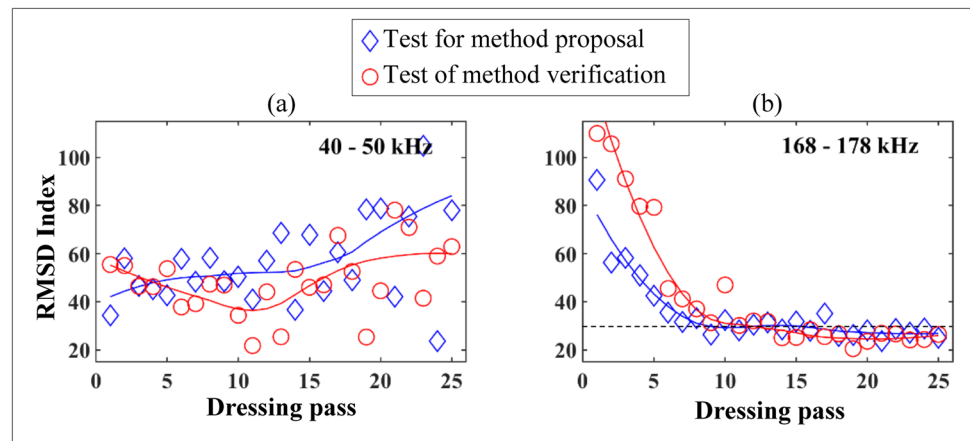


**Fig. 15** RMSD indices for the signals collected through the piezoelectric diaphragm: (a) 40–50 kHz; (b) 168–178 kHz



as the dressing process unfolds. This phenomenon is particularly pronounced within the frequency range of 182 to 192 kHz for the AE sensor and 168 to 178 kHz for the piezoelectric diaphragm. Figures 14b and 15b demonstrate a significant reduction in the damage index for the dressed grinding wheel condition compared to the undressed condition. This finding indicates a substantial decrease in cutting surface damage as the dressing progresses, ultimately stabilizing around a threshold value of 30. Consequently, this threshold value can effectively classify grinding wheels as dressed or undressed. In essence, a lower damage index reflects a diminished level of grinding wheel damage, signifying a regular and aggressive cutting surface.

When analyzing the results for both dressing conditions, a threshold equal to 30 can be defined to classify the wheel as dressed and undressed. Furthermore, this threshold can be applied to the AE sensor and the piezoelectric diaphragm. This means that the results are consistent and that even when using the methodology in different frequency ranges, the piezoelectric diaphragm was as efficient as the AE sensor in terms of classifying the cutting conditions of the grinding wheel throughout the dressing operation.

## 5 Conclusion

In this research, we propose a new method that utilizes piezoelectric sensors and a damage index to indirectly monitor the dressing operation and determine the transition point of the grinding wheel's cutting state based on a predefined threshold. The results demonstrate that applying the root mean square deviation (RMSD) index in frequency ranges directly associated with the grinding wheel's cutting conditions allows for establishing a threshold and classifying the wheel as dressed or undressed.

During our experiments, we observed that the optimal frequency range for the acoustic emission (AE) sensor was 182 to 192 kHz, while for the piezoelectric diaphragm, it was 168 to 178 kHz. Although different frequency ranges yielded the best results for each sensor, the defined threshold successfully classifies the grinding wheel's condition for both sensors. These findings affirm the potential of this novel non-invasive method to optimize the dressing operation of conventional grinding wheels, assist machine operators, and enhance the grinding process. Additionally, our results indicate that low-cost piezoelectric diaphragms can replace the traditional AE sensors commonly used in industrial applications without compromising the reliability of process-related data collection. Furthermore, it is worth noting that verifying this methodology ensures its reliability and can be extended to different types of grinding wheels, dressers, and variations of dressing parameters to enhance its robustness. Finally, it is advisable to investigate the specific boundaries of the frequency band to achieve accurate damage detection in grinding wheels. Additionally, exploring the potential applicability of the proposed methodology in diverse industrial contexts should be pursued. These investigations will contribute to advancing the understanding and implementation of the methodology in practical scenarios, thereby promoting progress in grinding wheel monitoring and optimization research. Moreover, optimizing the dressing process and investigating alternative sensors or transducers could further enhance the monitoring and control of grinding operations. Overall, this research establishes a foundation for advancing the field of monitoring dressing operations and optimizing grinding processes, paving the way for innovative approaches and future investigations.

**Acknowledgements** The authors would like to thank the Department of Electrical and Mechanical Engineering of the School of Engineering, Sao Paulo State University (UNESP), Bauru, São Paulo, and the Department of Electrical and Computer Engineering, São Carlos

School of Engineering, University of São Paulo, São Carlos, Sao Paulo, for providing the facilities and assets needed.

**Author contribution** All authors contributed to the study conception and design. Material preparation, data collection, and analysis were performed by Erick Luiz Vieira Ruas, Wenderson Nascimento Lopes, and Paulo Roberto Aguiar. The first draft of the manuscript was written by Erick Luiz Vieira Ruas, Wenderson Nascimento Lopes, Thiago Glissoi Lopes, and Pedro Oliveira Conceição Junior, and all authors commented on previous versions of the manuscript. All authors read and approved the final manuscript.

**Funding** The authors thank the CAPES (Coordination for the Improvement of Higher-Level Education Personnel) and CNPq (National Council for Scientific and Technological Development) for their financial support of this research through Grant # 306435/2017–9 and Grant # 306774/2021–6.

## Declarations

**Ethical approval** The manuscript contains original ideas which have never been published before in other journals.

**Consent to participate** Not applicable.

**Consent to publish** All the authors mentioned in the manuscript have agreed for authorship, read and approved the manuscript, and given consent for submission and publication of the manuscript.

**Competing interests** The authors declare no competing interests.

## References

- Black RA, Kohser JT (2008) DeGarmo's materials and processes in manufacturing, 10th ed. ed. River Street
- Nakai ME, Junior HG, Aguiar PR, Bianchi EC, Spatti DH (2015) Neural tool condition estimation in the grinding of advanced ceramics. *IEEE Lat Am Trans* 13(1):62–68. <https://doi.org/10.1109/TLA.2015.7040629>
- Patnaik Durgumahanti US, Singh V, Venkateswara Rao P (2010) A new model for grinding force prediction and analysis. *Int J Mach Tools Manuf* 50(3):231–240. <https://doi.org/10.1016/j.jmac.2009.12.004>
- Deng H, Xu Z (2019) Dressing methods of superabrasive grinding wheels: a review. *J Manuf Process* 45(March):46–69. <https://doi.org/10.1016/j.jmapro.2019.06.020>
- Wegener K, Hoffmeister HW, Karpuschewski B, Kuster F, Hahmann WC, Rabe M (2011) Conditioning and monitoring of grinding wheels. *CIRP Ann Manuf Technol* 60(2):757–777. <https://doi.org/10.1016/j.cirp.2011.05.003>
- Marinescu ID, Hitchiner M, Uhlmann E, Rowe WB, Inasaki I (2006) Handbook of machining with grinding wheels. *Handb Mach Grinding Wheels* 1–598. <https://doi.org/10.1201/b19462>
- Ribeiro DMS, Aguiar PR, Fabiano LFG, D'Addona DM, Baptista FG, Bianchi EC (2017) Spectra measurements using piezoelectric diaphragms to detect burn in grinding process. *IEEE Trans Instrum Meas* 66(11):3052–3063. <https://doi.org/10.1109/TIM.2017.2731038>
- Dornfeld D, Cai HG (1984) An investigation of grinding and wheel loading using acoustic emission. *J Eng Ind* 106(1):28–33. <https://doi.org/10.1115/1.3185907>
- Lopes WN et al (2021) An efficient short-time Fourier transform algorithm for grinding wheel condition monitoring through acoustic emission. *Int J Adv Manuf Technol* 113(1–2):585–603. <https://doi.org/10.1007/s00170-020-06476-3>
- LofranoDotto FR, Aguiar PR, Alexandre FA, Lopes WN, Bianchi EC (2020) In-dressing acoustic map by low-cost piezoelectric transducer. *IEEE Trans Ind Electron* 67(8):6927–6936. <https://doi.org/10.1109/TIE.2019.2939958>
- Lopes WN, Aguiar PR, Conceicao Junior PO, Dotto FRL, Fernandez BO, Bianchi EC (2021) Study of the use of piezoelectric diaphragm as a low-cost alternative to the acoustic emission sensor in dressing operation of aluminum oxide wheels. *IEEE Sens J* 21(16):18055–18062. <https://doi.org/10.1109/JSEN.2021.3085246>
- Lopes WN et al (2021) Method for fault detection of aluminum oxide grinding wheel cutting surfaces using a piezoelectric diaphragm and digital signal processing techniques. *Measurement (Lond)* 180(January). <https://doi.org/10.1016/j.measurement.2021.109503>
- Miranda HI, Rocha CA, Oliveira P, Martins C, Aguiar PR, Bianchi EC (2015) Monitoring single-point dressers using fuzzy models. *Procedia CIRP* 33:281–286. <https://doi.org/10.1016/j.procir.2015.06.050>
- Alexandre FA et al (2018) Tool condition monitoring of aluminum oxide grinding wheel using AE and fuzzy model. *Int J Adv Manuf Technol* 96(1–4):67–79. <https://doi.org/10.1007/s00170-018-1582-0>
- Lopes WN et al (2017) Digital signal processing of acoustic emission signals using power spectral density and counts statistic applied to single-point dressing operation. *IET Sci Meas Technol* 11(5):631–636. <https://doi.org/10.1049/iet-smt.2016.0317>
- Alexandre FA, Aguiar PR, Götz R, Viera MAA, Lopes TG, Bianchi EC (2019) A novel ultrasound technique based on piezoelectric diaphragms applied to material removal monitoring in the grinding process. *Sensors (Switzerland)* 19(18). <https://doi.org/10.3390/s19183932>
- Alexandre F et al (2018) Emitter-receiver piezoelectric transducers applied in monitoring material removal of workpiece during grinding process. 9. <https://doi.org/10.3390/ecs5-5-05732>
- Viera MAA et al (2019) Low-cost piezoelectric transducer for ceramic grinding monitoring. *IEEE Sens J* 19(17):7605–7612. <https://doi.org/10.1109/JSEN.2019.2917119>
- Inasaki I, Okamura K (1985) Monitoring of dressing and grinding processes with acoustic emission signals. *CIRP Ann* 34(1):277–280. [https://doi.org/10.1016/S0007-8506\(07\)61772-7](https://doi.org/10.1016/S0007-8506(07)61772-7)
- Martins CHR, Aguiar PR, Frech A, Bianchi EC (2013) Neural networks models for wear patterns recognition of single-point dresser. 46 (9. IFAC). <https://doi.org/10.3182/20130619-3-RU-3018.00222>
- Junior P, D'Addona D, Aguiar P, Teti R (2018) Dressing tool condition monitoring through impedance-based sensors: Part 2—Neural networks and k-nearest neighbor classifier approach. *Sensors* 18(12):4453. <https://doi.org/10.3390/s18124453>
- Lopes WN et al (2021) Method for fault detection of aluminum oxide grinding wheel cutting surfaces using a piezoelectric diaphragm and digital signal processing techniques. *Measurement* 180:109503. <https://doi.org/10.1016/j.measurement.2021.109503>
- Moia DFG, Thomazella IH, Aguiar PR, Bianchi EC, Martins CHR, Marchi M (2015) Tool condition monitoring of aluminum oxide grinding wheel in dressing operation using acoustic emission and neural networks. *J Braz Soc Mech Sci Eng* 37(2):627–640. <https://doi.org/10.1007/s40430-014-0191-6>
- Yang Z, Yu Z (2013) Experimental study of burn classification and prediction using indirect method in surface grinding of AISI 1045 steel. *Int J Adv Manuf Technol* 68(9–12):2439–2449. <https://doi.org/10.1007/s00170-013-4882-4>
- Rascalha A, Brandão LC, Filho SLMR (2013) Optimization of the dressing operation using load cells and the Taguchi method in the centerless grinding process. *Int J Adv Manuf Technol* 67(5–8):1103–1112. <https://doi.org/10.1007/s00170-012-4551-z>

26. Martins CHR, Aguiar PR, Frech A, Bianchi EC (2014) Tool condition monitoring of single-point dresser using acoustic emission and neural networks models. *IEEE Trans Instrum Meas* 63(3):667–679. <https://doi.org/10.1109/TIM.2013.2281576>
27. Junior P, D'Addona DM, Aguiar P, Teti R (2018) Dressing tool condition monitoring through impedance-based sensors: Part 2—neural networks and K-nearest neighbor classifier approach. *Sensors (Switzerland)* 18(12) <https://doi.org/10.3390/s18124453>.
28. Vaseghi SV (1996) *Advanced signal processing and digital noise reduction*. Vieweg+Teubner Verlag. <https://doi.org/10.1007/978-3-322-92773-6>
29. Solomon JOM (1991) *PSD computations using Welch's method*. [Power Spectral Density (PSD)]. Albuquerque, NM, and Livermore, CA (United States). <https://doi.org/10.2172/5688766>
30. De Castro BA, De MeloBrunini D, Baptista FG, Andreoli AL, Ulson JAC (2017) Assessment of macro fiber composite sensors

for measurement of acoustic partial discharge signals in power transformers. *IEEE Sens J* 17(18):6090–6099. <https://doi.org/10.1109/JSEN.2017.2735858>

**Publisher's note** Springer Nature remains neutral with regard to jurisdictional claims in published maps and institutional affiliations.

Springer Nature or its licensor (e.g. a society or other partner) holds exclusive rights to this article under a publishing agreement with the author(s) or other rightsholder(s); author self-archiving of the accepted manuscript version of this article is solely governed by the terms of such publishing agreement and applicable law.